J. Fluid Mech. (1972), *vol.* 54, *part* 2, *pp.* 351–367
Printed in Great Britain

Roll-diameter dependence in Rayleigh convection and its effect upon the heat flux

By G. E. WILLIS, J. W. DEARDORFF
National Center for Atmospheric Research, Boulder, Colorado
AND R. C. J. SOMERVILLE†
Courant Institute of Mathematical Sciences, New York University

(Received 7 September 1971 and in revised form 6 March 1972)

The average roll diameter in Rayleigh convection for $2000 < R < 31000$, where R is the Rayleigh number, has been measured from photographs of three convecting fluids: air, water and a silicone oil with a Prandtl number σ of 450. For air the average dimensionless roll diameter was found to depend uniquely upon R and to increase especially rapidly in the range $2000 < R < 8000$. The fluids of larger σ exhibited strong hysteresis but also had average roll diameters tending to increase with R. The increase in average roll diameter with R tended to decrease with σ. Through use of two-dimensional numerical integrations for the case of air it was found that the increase in average roll diameter with R provides an explanation for the usual discrepancy in heat flux observed between experiment and two-dimensional numerical calculations which prescribe a fixed wavelength.

1. Introduction

In Rayleigh convection between rigid horizontal plates held at constant temperatures, it is known that the convection occurs preferentially in the form of nearly two-dimensional rolls (Koschmieder 1966; Somerscales & Dropkin 1966; Rossby 1969; Krishnamurti 1970) for Rayleigh numbers somewhat supercritical. This result has been predicted by Schlüter, Lortz & Busse (1965) for the case when viscosity variations are relatively small. It is also known that the preferred wavelength L, which is twice the roll diameter, gives a close approximation to the critical value $\lambda_c = L_c/h = 2{\cdot}016$ for convection which is only slightly supercritical (Koschmieder 1966; Rossby 1969), where h is the separation between horizontal plates, λ is the dimensionless wavelength and the subscript c denotes the critical value at the onset of convection. What is not well known, however, is the dependence of the roll diameter upon R and σ, where R is the Rayleigh number and σ the Prandtl number, as R becomes increasingly supercritical. At sufficiently large values of R, of course, the convection patterns become too complicated and three-dimensional to allow identification of a preferred roll diameter,

† Present address: Goddard Institute for Space Studies, N.A.S.A., 2880 Broadway, New York 10025.

and at sufficiently large values of σ the dependence of the existing state of convection upon its history (Krishnamurti 1970) may become too great to allow any unique value for the preferred roll diameter to be determined.

Following the theory of Malkus (1954*a*), it has often been assumed that the preferred roll diameter for Rayleigh convection is that which maximizes the heat flux. Various theoretical studies have shown that this maximizing roll diameter *decreases* with increasing R. However, the experimental studies of Schmidt & Saunders (1938), Deardorff & Willis (1965), Koschmieder (1966), Rossby (1969) and Krishnamurti (1970) all seem to indicate that the preferred wavelength *increases* with R. (Although Foster (1969) found numerically that the preferred wavelength of steady rolls depends upon the initial conditions and does not generally maximize the heat flux, his study was two-dimensional and applicable only to large σ.) In view of this discrepancy more definitive measurements seem desirable so that the reason for the actual wavelength dependence can ultimately be understood.

While the influence of λ on the heat flux or Nusselt number N has not been studied extensively, numerical studies of two-dimensional convection using $\lambda = \lambda_c$ have given values of N too large by a significant fraction, compared with experimental values. The study of Lipps & Somerville (1971), using observed λ values for $\sigma = 100$, gave improved agreement (compared with results for constant λ) with Rossby's (1969) heat flux measurements for $\sigma = 200$. Even closer agreement between experimentally and numerically determined heat fluxes might have been expected if observed values of λ and N had been available for the same Prandtl number.

The purpose of this paper is to present experimental results on the dependence of λ upon R, σ and history within the domain for which the convection is mainly two-dimensional and, for the case of air, to investigate numerically the dependence of heat flux upon R and σ which is to be expected from the observed dependence of roll diameter.

2. Experimental equipment and techniques

The convection chamber has a square horizontal area 80×80 cm, a thick electrically heated aluminum base plate, and an upper glass plate which permits a top view of the convection. Cooling water circulates on top of the glass plate. For a more complete discussion of the equipment and associated experimental imperfections refer to Willis & Deardorff (1970).

Three fluids will be treated here: air ($\sigma = 0{\cdot}71$), water ($\sigma = 6{\cdot}7$) and a silicone oil having $\sigma = 450$. For air and silicone oil it was found satisfactory to use a glass plate of thickness 0·32 cm as the upper boundary, but for the case of water (which has a relatively large thermal conductivity) it was found necessary to use a very thin glass sheet of thickness 0·03 cm as the upper boundary.† This special glass necessitated the construction and use of a smaller rectangular chamber (31×69 cm). For support, the thin glass top was glued to ten equally spaced aluminum bars, each 0·32 cm wide, which lie parallel to the short side of

† Available from Corning Glass Works, Corning, N.Y.

the chamber and extend 1 cm into the water bath above. While these support bars are necessary to provide a nearly uniform chamber depth, they do cause some flow obstruction in the bath of circulating water. To minimize the resulting temperature fluctuations along the glass upper boundary, a greater circulation rate was used for this configuration. When the working fluid was air or silicone oil the circulating water in the cooling bath was given a depth of 2 cm and a flow rate of $0{\cdot}16\,l\,s^{-1}$; when the working fluid was water it was of depth 3·5 cm and had a flow rate of $0{\cdot}5\,l\,s^{-1}$.

The spacing h between horizontal plates was 2·54 cm for the case of air, 1·00 cm for the case of water and 1·05 cm for the silicone oil. The maximum temperature difference ΔT employed between the upper and lower plates was 30 °C for air, 2 °C for water and 17 °C for the silicone oil. The mean temperature within the chamber varied by no more than 0·5 °C during a given experiment of many hours duration and was maintained close to the room temperature. Horizontal variations of R were measured for the most critical experimental case of convection in water. Space–time variations in ΔT were $\pm 2\,\%$ on the average and $\pm 5\,\%$ at most. Spatial variations in h, associated with warping of the thin glass plate, averaged $\pm 1{\cdot}5\,\%$ and were at most $\pm 3\,\%$. Hence R varied locally in the horizontal by $\pm 6{\cdot}5\,\%$ on the average and by $\pm 14\,\%$ at most.

For flow visualization, an oil smoke composed of spherical particles was used in air. With this technique variations in smoke concentration allowed the convective patterns to be observed, as was discussed by Willis & Deardorff (1970). A small amount of flakes, which tend to align with fluid shear, was added to the liquids (a 'rheoscopic' fluid† to water and graphite particles in the silicone oil) to make convection patterns visible. Slit lighting from the side was used, with the upper half to three-quarters of the chamber depth being illuminated.

Average roll diameters were determined from top-view photographs of the convective patterns. The diameters of curved rolls and occasional cells, as well as nearly straight rolls, were included in the average values. Spatial averaging was necessary because of the irregular shapes of the convection rolls and the large variation in their diameters from point to point. The spatial averaging was accomplished by dividing the photographed area into a uniform grid and measuring the roll diameter centred at each grid point. The area of the convection chamber treated in each case is denoted in figure 1 by the region enclosed within the dashed lines. The regions were selected by virtue of better illumination, greater photographic contrast and unobstructed visibility from the top, and not because of any spatial difference in roll structure. The percentage of the chamber area treated in the data analysis is approximately 35% for air, 80% for water and 30 % for the silicone oil. Photographs of the convective patterns which appear in this paper are of the entire data regions for the cases of air and water and of about half the data region for the case of the silicone oil.

† Available from Kalliroscope Corporation, Cambridge, Massachusetts.

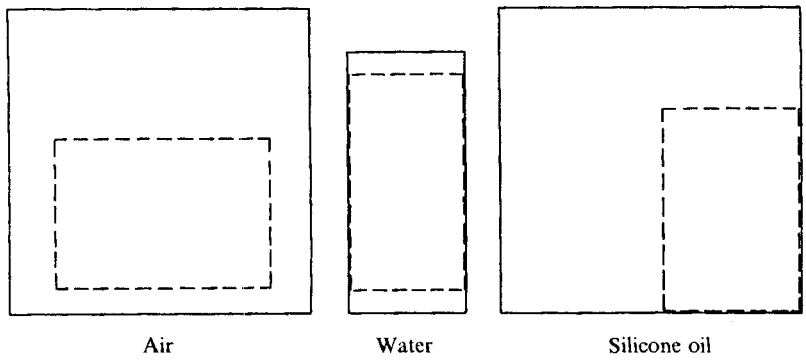

FIGURE 1. Photographed regions of the convection chamber used in the data analysis (enclosed by dashed lines) in relation to the convection chamber total area (enclosed by solid lines) for the three fluids investigated. (*a*) Air. (*b*) Water. (*c*) Silicone oil.

3. Dependence of λ upon R

3.1. *Small* σ *(air)*

For the case of air, the fluid was found to be capable of selecting a unique average roll diameter without appreciable hysteresis (at least for $(h^2/\kappa)\,|\partial R/\partial t| < 30$, where κ is the thermal diffusivity) because of the occurrence of time-dependent motions even at small R, as described by Willis & Deardorff (1970). In the present experiments R was increased in increments of about 1000. After such a change R was maintained constant for a period of about 30 min; then smoke particles were introduced from one corner of the chamber, after which an adjustment period of about 10 min for $R < 5000$ or 5 min for $R > 6000$ was allowed for a new fluid equilibrium to be achieved. Then a photograph of the convective patterns was taken and 2 min later a second photograph was taken. The smoke was then removed from the chamber and the above procedure repeated for the next higher value of R.

The results of the analysis of the photographs using this procedure are shown in figure 2 by the solid circles, which represent the average λ values $\overline{\lambda}$. Each solid circle represents the average of about 165 individual measurements of λ for $R < 10000$ and about 100 for $R > 10000$. The standard deviation of the mean, a measure of the variability of the sample means, is denoted by the error bars at various values of R. The standard deviation of the individual dimensionless roll diameters, a measure of the spatial variability of roll size, ranged from 0·25 at $R = 2500$ to 0·61 at $R = 28000$. Thus, at the latter value of R, for example, where $\overline{\lambda} \approx 4{\cdot}2$, for a Gaussian distribution we expect to find wide rolls with $\lambda \geqslant 4{\cdot}8$ covering about 16 % of the area of a large convection chamber and narrow rolls with $\lambda \leqslant 3{\cdot}6$ occupying another 16 %, while the actual area occupied by each was about 17 %.

The rapid increase of $\overline{\lambda}$ with R as R first exceeds $R_c = 1708$ is very pronounced. The data points in this region extrapolate well to a value $\lambda_c = 2{\cdot}016$, shown in the figure by the open circle. Also apparent is a change to less rapidly increasing $\overline{\lambda}$ values for $R \gtrsim 8000$. The reason for this change is not known, although it has

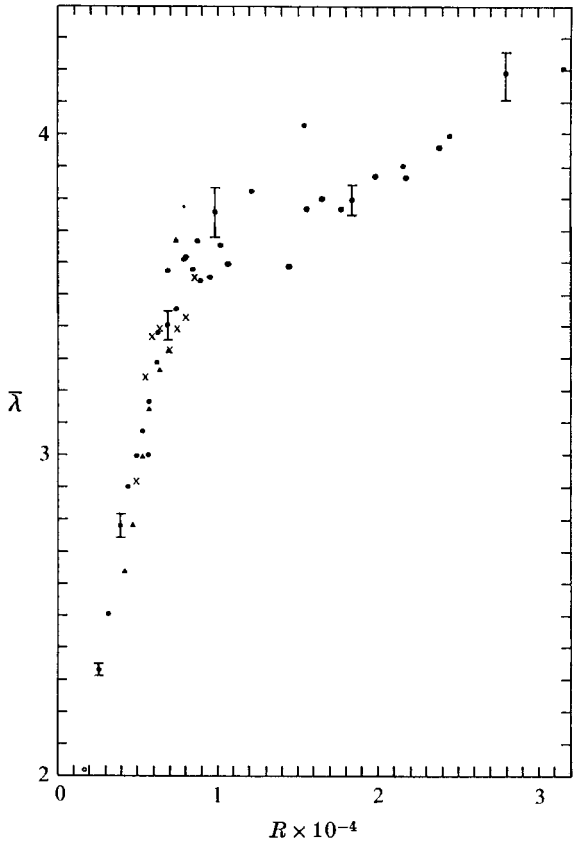

FIGURE 2. Non-dimensional roll diameter as a function of Rayleigh number in air ($\sigma = 0{\cdot}71$). ○, theoretical λ_c value at R_c; ●, R held constant with a fresh supply of tracer introduced into the chamber, 5 or 10 min elapsing before photographs were taken, for each value of constant R; ▲, R continuously increased, using a single supply of smoke initially introduced at $R = 4200$ to serve as the flow tracer; ×, R continuously decreased, using a single supply of smoke initially introduced at $R = 8600$.

been suggested by F. Busse and F. Lipps (private communications) that it may be associated with the roll waviness (Willis & Deardorff 1970) and accompanying three-dimensional disturbances which commence with small amplitude at $R \approx 5800$. Relatively large amplitude is attained when $R \gtrsim 8500$. The implications of the pronounced change in $\bar{\lambda}$ near $R = 8000$ upon the heat flux will be discussed in the next section.

Some other experiments were performed using a different method to test the hypothesis that these average λ values are unique, i.e. independent of the history of the motion if R is held approximately constant for a period exceeding about $5h^2/\kappa$. The smoke tracer was admitted to the chamber at $R = 4200$ and was left undisturbed as R was increased continuously to 7500 at a rate corresponding to $\partial(\Delta T)/\partial t = 4{\cdot}1\,^\circ\mathrm{C/h}$. Similarly, smoke admitted at $R = 8600$ was left undisturbed as R was decreased to 4800 at a rate corresponding to $3{\cdot}5\,^\circ\mathrm{C/h}$. The data points for $\bar{\lambda}$ obtained in each manner are shown in figure 2 by solid triangles and crosses, respectively. No systematic differences occur between the R-increasing and

R-decreasing values of $\bar{\lambda}$. Also these $\bar{\lambda}$ values are in good agreement with those from the previous experiments in which R was held constant and the fluid was undisturbed for periods of 7–12 min.

3.2. *Moderately large σ (water)*

For the case of water, the fluid was found incapable of selecting a unique average roll diameter at the R values examined ($2000 < R < 34\,000$) over time periods at least as long as $30h^2/\kappa$ or $200h^2/\nu$, where ν is the kinematic viscosity. Instead, a dependence upon the history was found. To demonstrate this behaviour separate experiments were performed, one with R increasing and one with R decreasing. In the former case R was increased continuously at a rate corresponding to $\partial(\Delta T)/\partial t = 0{\cdot}3\,^{\circ}\mathrm{C/h}$ after first allowing sufficient time for rolls to become well established at $R \simeq R_c$. In the latter case R was increased rather quickly to 34 000, maintained at that value for 2 hours and then allowed to decay gradually at a rate corresponding to $0{\cdot}3\,^{\circ}\mathrm{C/h}$. In both cases photographs of the convection patterns were taken in R increments of about 1000 and then analysed in a manner similar to the case of air. Each data point represents the average of about 150 individual measurements of λ. The results are shown in figure 4, where the standard deviation of the mean is denoted by the error bars at various values of R. The standard deviation of the individual dimensionless roll diameters ranged from 0·33 at $R = 3400$ to 0·91 at $R = 25\,400$. For the R-increasing experiment, smaller values of $\bar{\lambda}$ existing initially at small R are seen to tend to persist as R increases. Larger values of $\bar{\lambda}$, existing at the beginning of the decay experiment, are seen to tend to persist as R is subsequently decreased.

No abrupt change in $\partial\bar{\lambda}/\partial R$ for water is evident in figure 4. However, a gradual change in $\partial\bar{\lambda}/\partial R$ appears to be centred at $R \approx 16\,000$ for the R-increasing case and at $R \approx 11\,000$ for the R-decreasing case. This gradual change may be associated with the gradual appearance (or disappearance) of three-dimensional banded structures having the rectangular or bimodal appearance predicted by Busse (1967) for large σ, and further described by Busse & Whitehead (1971). The superposition of the new structures on the existing rolls is shown for the R-increasing case in the sequence of photographs of figure 5 (plate 2). They developed preferentially upon rolls having relatively greater diameters and straighter outlines, and could first be perceived at $R \approx 11\,000$ as R increased (see figure 5(*b*)), or last discerned at $R \approx 8000$ as R decreased. Their relative abundance gradually increased as R approached 23 000, at which value they occupied about 75 % of the area. The remaining area was occupied by rolls of strong curvature and by large irregular cells.

Bimodal convection probably would have occupied all of the area if initially only straight rolls had been present (Busse & Whitehead 1971). Instead, the convective pattern just before the start of the increase in R was as in figure 5(*a*). The numerous small cells and roll segments are remnants of small cells formed at the onset of convection (Somerscales & Dougherty 1970). Only after a considerable time lapse and for a somewhat supercritical R did the cells evolve into irregular rolls. The more irregular patterns tend to be 'squeezed out' by the more regular rolls, as will be discussed in § 5.

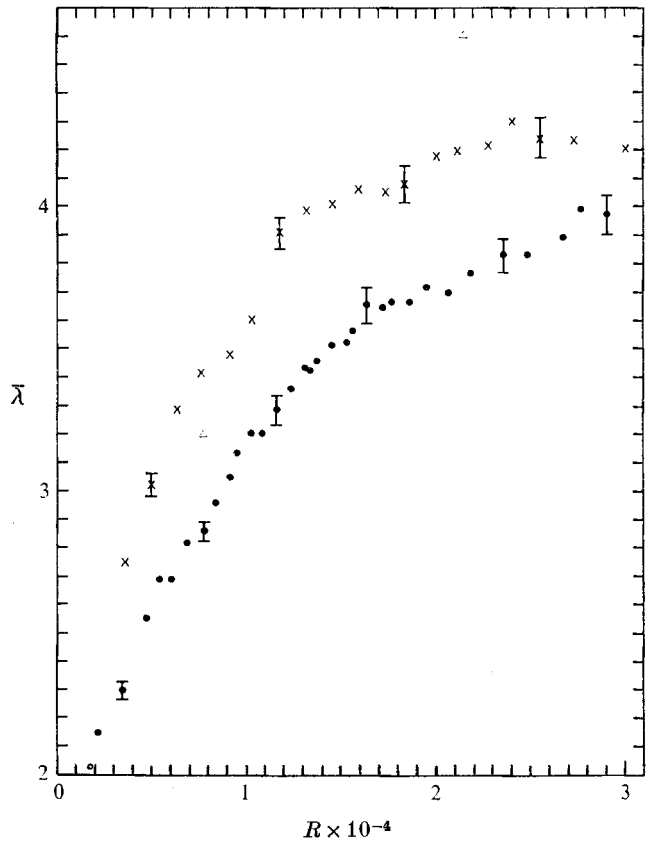

FIGURE 4. Non-dimensional roll diameter as a function of Rayleigh number in water ($\sigma = 6{\cdot}7$). ○, λ_c value at R_c; ●, R continuously increasing; ×, R continuously decreasing; △, R held constant, with the fluid being stirred initially and the convection patterns allowed to evolve over a 4 hour period.

Two additional $\bar{\lambda}$ values shown in figure 4 by triangles were obtained by a method more similar to that used in air. In each case R was held fixed, the fluid was stirred by passing a long rod through it, and photographs were taken periodically as the fluid convective pattern approached a new equilibrium. The results of this experiment are shown in figure 6. About 90 % of the increase in $\bar{\lambda}$ (from a value less than 2·0 immediately after stirring) was attained after about 30 min, which is a period of about $3h^2/\kappa$. The average λ was still slowly changing after 4 h. The 'final' $\bar{\lambda}$ value for $R = 7700$ lies between the values resulting from the R-increasing and R-decreasing experiments. The convective pattern in all three cases consisted mainly of rolls with a few cells present. The 'final' $\bar{\lambda}$ value for $R = 21400$ is considerably larger than the value for either the R-increasing or the R-decreasing experiment. This results from the presence of increased numbers of large irregular cells, which covered about 70 % of the area. The variability of $\bar{\lambda}$ for these two values of R, and for the three different sets of 'initial conditions', demonstrates its history dependence in water.

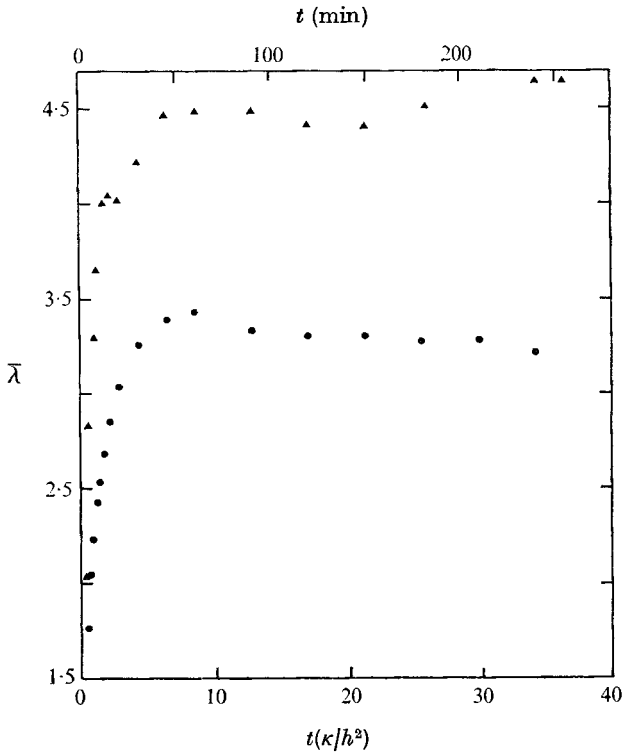

FIGURE 6. Non-dimensional roll diameters in water as a function of time, with fluid stirred at time $t = 0$. ●, $R = 7640$; ▲, $R = 21400$.

3.3. *Large* σ (*silicone oil with* $\sigma = 450$)

For the case of the silicone oil the hysteresis is even more pronounced than in water at small R, as is shown by figure 7. These data were collected in the following manner. The Rayleigh number R was increased from R_c to about 5000 and then maintained constant for a time sufficient to allow the rolls to become well established. A photograph was then taken, after which R was increased by about 2000 over a period of about 10 min. R was kept at this new value for about 30 min (about $2h^2/\kappa$), after which another photograph of the convective pattern was taken. The above procedure was repeated until $R = 34000$. The final condition of the R-increasing experiment served as the initial condition for the R-decreasing experiment. Data in the latter case were taken in a similar manner. The photographs of the convection patterns were analysed in a manner similar to that described for air. Each data point represents the average of about 175 individual measurements of λ. The standard deviation of the mean is denoted by the error bars at various values of R; the standard deviation of the individual dimensionless roll diameters ranged from 0·19 at $R = 5200$ to 0·35 at $R = 29300$.

There is a rather pronounced change in $\partial\bar{\lambda}/\partial R$ shown in figure 7 for R gradually *increasing*, for $1{\cdot}5 \times 10^4 < R < 2{\cdot}0 \times 10^4$. These approximate limits correlate well with the R values at which the bimodal convection was first noticed to occur in a few selected regions and at which it occupied the entire area, respectively.

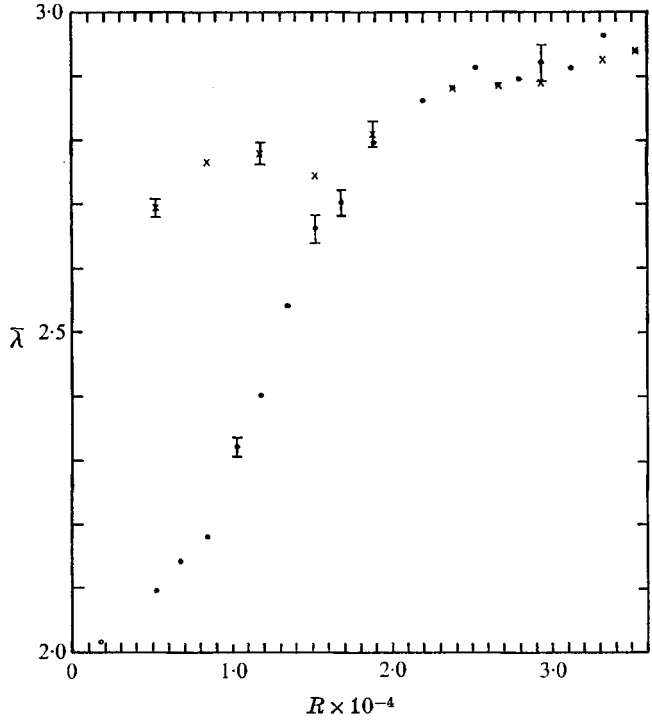

FIGURE 7. Non-dimensional roll diameter as a function of Rayleigh number in silicone oil with $\sigma = 450$. ○, value of λ_c; ●, R increasing; ×, R decreasing.

These limits depend upon the diameters of the rolls on which the second convective mode formed, however, and are therefore history dependent. The lack of any pronounced change in $\partial\bar{\lambda}/\partial R$ for the R-decreasing case is evident in figure 7.

The appearance of the convection patterns in the silicone oil at four different Rayleigh numbers is shown in figure 8 (plate 3). The photographs are from an R-increasing experiment. The preference of the second mode to develop on the wider rolls is evident, as is the retreat of rolls with pinched ends.

An unanswered question suggested by figures 4 and 7 concerns how long one must wait, in terms of days, weeks or months, before a $\bar{\lambda}$ value for $R_c < R < 20000$ obtained from one set of initial conditions agrees with one obtained from a distinctly different set.

3.4. *Dependence of* $\bar{\lambda}$ *upon* σ

For illustration purposes smooth curves drawn through the data points of figures 2, 4 and 7 appear in figure 9 along with the error limits of the sample means. Values of $\bar{\lambda}$ for $\sigma = 450$ are considerably smaller than those for the other two fluids studied. The $\bar{\lambda}$ values for the R-increasing and R-decreasing cases of water tend to enclose the $\bar{\lambda}$ values for air. As previously noted, the large values of $\bar{\lambda}$ for the R-decreasing case for water are due to the abundance of large cells during the initial stages of the decay.

It is appropriate here to compare results of experiments which are not highly dependent on initial conditions, or which have similar initial conditions. The

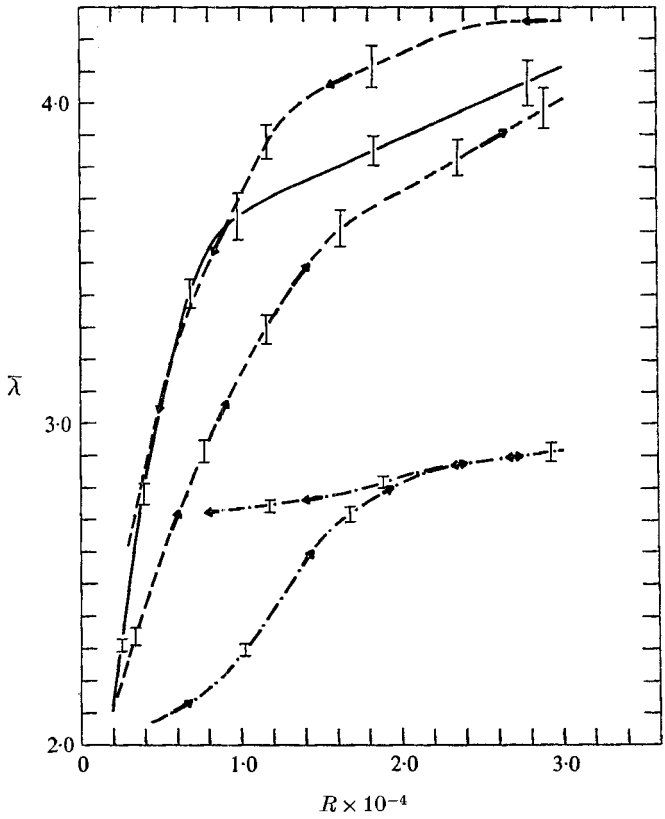

FIGURE 9. Smoothed values of non-dimensional roll diameter, with error limits, taken from figures 2, 4 and 7. ——, $\sigma = 0{\cdot}71$; – – →, $\sigma = 6{\cdot}7$, R increasing; – – ←, $\sigma = 6{\cdot}7$, R decreasing; –·–·→, $\sigma = 450$, R increasing; –·–·←, $\sigma = 450$, R decreasing.

R-increasing experiments for water and the silicone oil had similar initial conditions, i.e. essentially two-dimensional rolls were the dominant form of convection, while it has been shown earlier that our $\bar{\lambda}$ values for air are not dependent on initial conditions. Comparison of these three curves, along with consideration of their respective error estimates, indicates that $\partial\bar{\lambda}/\partial R > 0$ and $\partial(\partial\bar{\lambda}/\partial R)/\partial\sigma < 0$ within the Rayleigh number region for which the convective flow is mainly two-dimensional. These results are in qualitative agreement with those of Krishnamurti (1970).

One uncertainty regarding these conclusions (especially for large σ) results from lack of knowledge about the effect on $\bar{\lambda}$ of gradual changes in R.

4. Influence of $\bar{\lambda}$ upon heat flux

The observed dependence of $\bar{\lambda}$ upon R must influence measured values of the heat flux or of the Nusselt number N. To the extent that the convection is described by the usual Boussinesq equations and consists of rolls which are nearly straight, two-dimensional numerical studies could determine the dependence of

N upon R if $\bar{\lambda}(R)$ were specified correctly. Discrepancies between numerical and experimental results could signify the occurrence of three-dimensional structures which transport significant amounts of heat or which affect the rate of heat transport by coexisting with two-dimensional rolls.

Two specific questions arise with respect to the dependence of $\bar{\lambda}$ upon R and of N upon $\bar{\lambda}$. First, could the systematic increase of $\bar{\lambda}$ with R account for measurements of an approximately linear increase of NR with R, for the small R values considered here? Such linearity was found by Malkus (1954*b*), Willis & Deardorff (1967) and Krishnamurti (1970) between discrete transitions in $\partial(NR)/\partial R$. In contrast, numerical integrations of Deardorff (1968) and others have shown that if $\bar{\lambda}$ is held fixed NR will increase with R more rapidly than linearly in two-dimensional convection. Thus, the possibility exists that an increase of $\bar{\lambda}$ with R will counteract this nonlinearity so as to cause NR to increase nearly linearly from R_c to R_2, where R_2 is the Rayleigh number of the first supercritical heat flux transition. Second, could the pronounced change in $\partial\bar{\lambda}/\partial R$ observed in air for $7000 < R < 10000$ cause the heat flux transition observed at $R \approx 8200$ by Willis & Deardorff (1967)? Similarly, would the less abrupt change in $\partial\bar{\lambda}/\partial R$ observed in water and for $\sigma = 450$ with R increasing cause a similar but less pronounced heat flux transition? Krishnamurti (1970) has associated the appearance of bimodal convection with the heat flux transition at R_2. Our observations in water and silicone oil indicate good correlation between changes in $\partial\bar{\lambda}/\partial R$ and the appearance or disappearance of bimodal convection. Thus the possibility exists that the change in $\partial\bar{\lambda}/\partial R$ and/or the presence of bimodal convection could cause the transition at R_2.

To help answer such questions one of us (Somerville 1970) has developed an interpolation formula for N from two-dimensional numerical integrations. The numerical model used is reported in Lipps & Somerville (1971). The formula, which clearly shows the effect of $\bar{\lambda}$ upon N, made use of the results from about sixty distinct integrations and is given by

$$N = [R/R_c]^{0\cdot385+0\cdot9(R_c/R)} + 0\cdot01[R/R_c - 1][\delta + 2\cdot3(2-\bar{\lambda})(1+\tfrac{1}{3}\delta)], \qquad (1)$$

where $\delta = 1$ for $\sigma = 0\cdot71$ and 0 for $\sigma \geqslant 6\cdot8$. Somewhat different forms of the exponent could be used for compatibility with existing theoretical results, but the exponent given seems to be the simplest good fit to the numerical data. The accuracy of interpolation is within about $\pm 2\%$, but only for the conditions $\sigma = 0\cdot71$ or $\sigma \geqslant 6\cdot8$, $R < 22600$ and $2\cdot02 < \bar{\lambda} < \lambda_B(R)$, where $\lambda_B(R)$ is the maximum wavelength allowed by Busse's (1967) theory. Outside these parameter ranges the formula is inaccurate and a numerical model must be employed. Therefore, in this paper direct numerical integrations were employed instead of formula (1). In the integrations no attempt was made to model the variability in λ existing at a given value of R; only a single value of $\bar{\lambda}$ was prescribed for each value of R.

4.1. *Small σ (air)*

The numerical programme was applied for $\sigma = 0\cdot71$ using $\bar{\lambda}$ values obtained from figure 2. The values of NR which resulted are shown in figure 10 by the solid curve, along with the values which result if $\bar{\lambda}$ is constrained to be constant

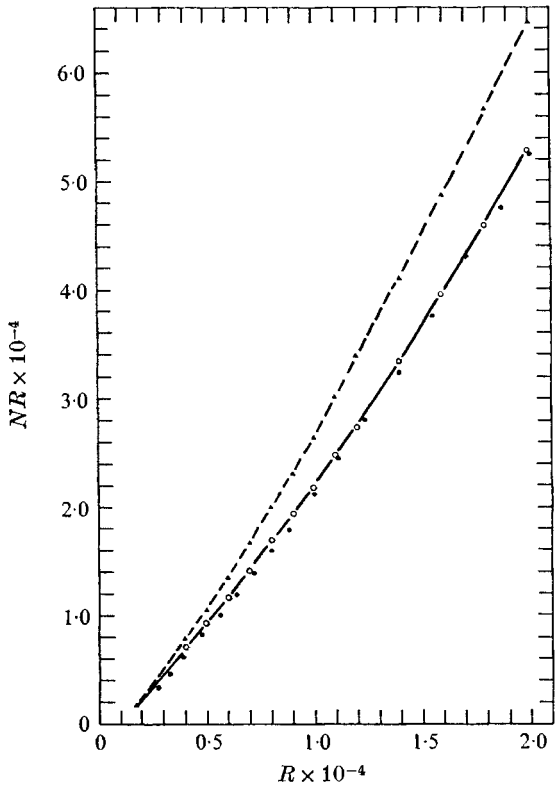

FIGURE 10. Measured and numerically calculated values of NR as a function of R for air (σ = 0·71). Numerical results: ——○——, variable λ as observed in air; – – ▲ – –, constant λ = 2·0. Experimental results: ●, Willis & Deardorff (1967) run B.

at $\bar{\lambda}$ = 2·0 (dashed curve) and the measured values of Willis & Deardorff (1967) for their run B. The use of the numerical programme itself rather than the formula above is necessary because $\bar{\lambda} > \lambda_B(R)$. The heat flux measurements of run B of Willis & Deardorff are used for comparison here since their absolute values are more accurate than those of run A. However, the accuracy of measurement of R was greater for run A.

The calculated NR values using the realistic $\bar{\lambda}$ data lie much closer to the measured values than do those for the fixed $\bar{\lambda}$ of 2·0. However, they indicate a gradual change in the slope of the NR *vs.* R curve and do not show any definite transition at $R \approx 8000$. This result appears to be associated with the fact that the dependence of N upon $\bar{\lambda}$ is rather weak, and that the change of $\partial\bar{\lambda}/\partial R$ with R is not perfectly abrupt at $R \approx 8000$. The existence of a heat flux transition in air for R near 8000 is still rather controversial, but has recently been confirmed by W. Brown (M.I.T., Department of Meteorology, private communication). We can only conclude from these considerations that whatever mechanism causes the heat flux transition is also responsible for the decreased dependence of $\bar{\lambda}$ upon R for $R > 8000$.

The general agreement of the numerical results with the experimental ones

from run B, using approximately correct $\bar{\lambda}$ values in the numerical programme, implies that whatever structure causes the observed behaviour in $\bar{\lambda}$ for $R > R_2 \approx 8000$ does not, by itself, strongly affect the heat transport.

4.2. *Moderate* σ (*water*, $\sigma = 6{\cdot}7$) *and large* σ (*silicone oil*, $\sigma = 450$)

Although no heat flux measurements or numerical calculations with appropriate $\bar{\lambda}$ values were made for the cases of water and silicone oil, it is interesting to compare the results of our wavelength data with the heat flux measurements of others.

The R-increasing values of $\bar{\lambda}$ from figure 4 display a change in slope at $R \approx 16000$. This value compares favourably with Krishnamurti's (1970) measured value of $R_2 \approx 17000$ for water. The R-decreasing values of $\bar{\lambda}$ from figure 4 indicate a change in slope at $R \approx 11000$; for decay experiments in water Malkus (1954*b*) occasionally observed a value of R_2 as small as 10000. For large σ and the R-increasing case, figure 7 shows a change in slope of the $\bar{\lambda}$ *vs.* R curve at $R \approx 20000$. For comparably large values of σ Krishnamurti (1970) observed a value of $R_2 \approx 22000$. The R-decreasing values of $\bar{\lambda}$ from figure 7 indicate no significant change in slope. In a decay experiment with $\sigma = 8500$ Krishnamurti (1970) found no heat flux transition in the range $5000 < R < 27000$.

The general agreement between our values of R for which $\partial\bar{\lambda}/\partial R$ exhibits a pronounced change and R_2 values of others, although suggestive, is not conclusive. The history dependence of $\bar{\lambda}$ and R_2 for moderate and large σ makes comparisons between experiments of various workers somewhat tenuous. Measurements of both wavelength and heat flux during the same experiment would be desirable.

The evidence that $R_2 \approx 8200$ in air, 11000–16000 in water and 21000 or so for $\sigma = 450$ casts doubt upon the results of run E of Willis & Deardorff (1967). Results of this run indicated the transition $R_2 \approx 8200$ was present for $\sigma = 57$ when R was slowly increased with time. No heat flux transition at such a relatively small R was found in Krishnamurti's (1970) test of fluids with comparably large σ. Thus it would be of considerable interest if future studies could clarify the σ dependence of R_2.

5. Roll-diameter selection mechanisms

For the fluids we have studied, we find that a primary mechanism whereby existing rolls can *increase* in diameter is through the retreat of a nearby roll which terminates in a pointed or pinched end. Several examples of such rolls is evident in figure 5 (plate 2). This mechanism has also been observed and described by Busse & Whitehead (1971). In our experiments many of these features were initially present in the interior of the chamber and thus provided a ready mechanism for $\bar{\lambda}$ to change relatively rapidly with R or with time at small R. If one were to begin an experiment with straight rolls of stable wavelength imposed across the entire width of the chamber $\bar{\lambda}$ would probably change only slightly with R, if at all, since pinched rolls would then be very infrequent.

Never have we observed a roll with one pinched end to advance. Upon retreat, neighbouring rolls expand into the extra space available, so that the average λ

increases. At moderate and large σ this mechanism is more important when R is increased slowly than when R is decreased slowly; for in the former case there are usually more irregular rolls at a given R owing to a history of cells, short roll segments, and randomly oriented longer rolls which formed soon after the fluid first became convective. In the latter case, the pinched rolls have had greater opportunity and longer time to retreat into short roll segments having both ends pinched and finally to vanish altogether.

For $\sigma = 0{\cdot}71$ the motion is sufficiently unsteady for this mechanism to be equally operative whether R is increased slowly or decreased slowly. At this σ we have been able to observe that, as a pinched roll end retreats, fluid actually flows or spirals along the length of the roll away from the retreating end. That is, a vertically integrated net flow then exists at right angles to the plane containing the main convective motion. This observation suggests that the occurrence of Busse's second mode of convection superimposed upon the rolls would hinder such longitudinal flow and would help to stabilize $\bar{\lambda}$. This conclusion is consistent with the $\bar{\lambda}$ versus R curves of figures 4 and 7 for moderate and large σ respectively. It is also consistent with observations of the rate of retreat of pinched roll ends which were identifiable both before and after the appearance of the second mode, for $\sigma = 450$. The average rate of retreat between successive Rayleigh numbers in figure 7 was $0{\cdot}67h\,\mathrm{h}^{-1}$ for $R < R_2$, while it was $0{\cdot}21h\,\mathrm{h}^{-1}$ for $R > R_2$. It should be stated, however, that no vertically integrated flows have been observed at large σ and that such a mass-transfer mechanism cannot be operative within a roll having both ends pinched.

An observed mechanism whereby rolls can shrink in diameter is the formation of a new cell or blob, which usually elongates or amalgamates into a curved roll. Neighbouring rolls are thereby decreased in diameter through direct transfer of fluid into the growing cell via the down-draft (for example) forming the outer edge of a growing cell with up-draft at its centre. The down-draft in this case has been observed to tilt inwards towards the cell centre as one looks downwards in the fluid, and conversely if the cell edge is an up-draft. This mechanism occurs rather frequently in air (Willis & Deardorff 1970), less frequently in water, and has not been observed at $\sigma = 450$.

Another mechanism observed in water whereby $\bar{\lambda}$ can decrease is the division of a large cell into two or more smaller cells which subsequently elongate into roll segments. The only roll-shrinking mechanism we have observed at very large σ operates in the approximate range $8000 < R < 22\,000$, where Busse's second mode selectively disappears as R is slowly decreased. In this case, the rolls which survive usually lie at right angles to the original rolls and have smaller diameters because the second mode has a smaller wavelength than the original rolls (see figure 5).

An additional roll-shrinking mechanism at large σ has been reported by Busse & Whitehead (1971) for $R_c < R < 8000$. Rolls with diameters unstably large develop a wavy pattern on a large scale, with crests and troughs lying along lines oriented at some acute angle to that of the original rolls. New rolls of smaller diameter gradually form along these lines while the original rolls disappear.

All of these complicated mechanisms which can change the diameters of rolls

imply the existence of structure which is three-dimensional. This conclusion agrees with earlier findings of Deardorff & Willis (1965) that, in convection which is constrained to be nearly two-dimensional (by placing two of the side walls close together), the wavelength is not free to vary with R. The equivalent conclusion was reached numerically by Lipps & Somerville (1971).

The theoretical studies of Davis (1968) and Nield (1968) present mechanisms (side wall effects and finite thermal conductivity of the top boundary, respectively) which lead to predictions of $\lambda > \lambda_c$ for R slightly supercritical. The relevance of these mechanisms in our experiments has been considered.

Examination of the raw wavelength data indicates no systematic tendency for rolls of larger diameter to be located nearer the walls. Roll diameters are variable throughout the chamber, with deviations from the mean as large as $\pm 50\,\%$, at least for small and moderate Prandtl numbers. Also, the formation and retreat of pinched-end rolls (the primary observed mechanism for the increase of $\bar{\lambda}$) has been observed to occur more frequently within the interior of the fluid than close to the side walls. In view of these results and of the relatively large convection-chamber aspect ratios (31:1 for air and water, 76:1 for silicone oil), it does not appear that the side wall mechanism could account for our observed increase of $\bar{\lambda}$ with R. Nor does it appear that the effect of finite thermal conductivity of the upper glass plate alone could account for the observed increase of $\bar{\lambda}$ with R. Krishnamurti's (1970) observations of such increase were obtained in a chamber in which both upper and lower plates consisted of thick aluminum blocks.

6. Summary and conclusions

(i) The dependence of the average roll diameter upon Rayleigh number has been documented for air for $R_c < R < 31\,000$. The rate of increase is very pronounced for $R < 7000$ or 8000 and much less pronounced in the remainder of the range. The increase contradicts those theoretical studies which have predicted or assumed that the dominant roll diameter is constant or decreases with increasing R.

(ii) For $\sigma = 6{\cdot}7$ or 450, a similar but somewhat less pronounced dependence of roll diameter upon R occurs which, however, is dependent upon history, at least for $R_c < R < 22\,000$.

(iii) Numerical calculations of the heat flux in air give much closer agreement with experimental measurements when observed $\bar{\lambda}$ values are used rather than with a constant $\bar{\lambda}$ value of 2·0. However, they did not reproduce a definite heat flux transition near $R = 8000$.

(iv) The Rayleigh number region in which $\partial\bar{\lambda}/\partial R$ undergoes a decrease correlates well with the value of R of the first supercritical heat flux transition. For air this decrease in $\partial\bar{\lambda}/\partial R$ may possibly be associated with a roll waviness which attains significant amplitude near $R = 8000$ and which could slightly enhance the heat flux. For the fluids with larger σ investigated, the decrease in $\partial\bar{\lambda}/\partial R$ and the first supercritical heat flux transition are apparently associated with the occurrence of bimodal convection. The earlier measurement (Willis &

Deardorff 1967) of a heat flux transition at $R \approx 8000$ at rather large σ now appears anomalous.

(v) The mechanisms whereby rolls change their diameters involve the complexities of unsteady three-dimensional motions, irregular shapes of rolls and cells, and, at least at small σ, net spiralling flow of fluid within a roll. Only three-dimensional numerical integrations seem capable of treating such complications rigorously.

(vi) For all fluids investigated it was found that $\partial\bar{\lambda}/\partial R > 0$ and $\partial(\partial\bar{\lambda}/\partial R)/\partial\sigma < 0$ within the Rayleigh number regions where the flow is mainly two-dimensional.

The work of one of us (R.C.J.S.) has been supported by the U.S. Atomic Energy Commission under contract AT(30-1)-1480 with the Courant Institute of Mathematical Sciences and, at the Summer Program in Geophysical Fluid Dynamics at the Woods Hole Oceanographic Institution, by the National Science Foundation under NSF Grant GJ-133. Significant improvements in the paper resulted from consideration of a referee's comments concerning inclusion of error limits of the roll diameters. The National Center for Atmospheric Research is sponsored by the National Science Foundation.

REFERENCES

Busse, F. H. 1967 On the stability of two-dimensional convection in a layer heated from below. *J. Math. Phys.* **46**, 140–150.

Busse, F. H. & Whitehead, J. A. 1971 Instabilities of convection rolls in a high Prandtl number fluid. *J. Fluid Mech.* **47**, 305–320.

Davis, S. H. 1968 Convection in a box: on the dependence of preferred wavenumber upon the Rayleigh number at finite amplitude. *J. Fluid Mech.* **32**, 619–624.

Deardorff, J. W. 1968 Examination of numerically calculated heat fluxes for evidence of a supercritical transition. *Phys. Fluids*, **11**, 1254–1256.

Deardorff, J. W. & Willis, G. E. 1965 The effect of two-dimensionality on the suppression of thermal turbulence. *J. Fluid Mech.* **23**, 337–353.

Foster, T. D. 1969 The effect of initial conditions and lateral boundaries on convection. *J. Fluid Mech.* **37**, 81–94.

Koschmieder, E. L. 1966 On convection on a uniformly heated plane. *Beit. Z. Phys. Atmos.* **39**, 1–11.

Krishnamurti, R. 1970 On the transition to turbulent convection. Part 1. The transition from two- to three-dimensional flow. *J. Fluid Mech.* **42**, 295–307.

Lipps, F. B. & Somerville, R. C. J. 1971 Dynamics of variable wavelength in finite-amplitude Bénard convection. *Phys. Fluids*, **14**, 759–765.

Malkus, W. V. R. 1954*a* Discrete transitions in turbulent convection. *Proc. Roy. Soc.* A **225**, 185–195.

Malkus, W. V. R. 1954*b* The heat transport and spectrum of thermal turbulence. *Proc. Roy. Soc.* A **225**, 196–212.

Nield, D. A. 1968 The Rayleigh–Jeffreys problem with boundary slab of finite conductivity. *J. Fluid Mech.* **32**, 393–398.

Rossby, H. T. 1969 A study of Bénard convection with and without rotation. *J. Fluid Mech.* **36**, 309–335.

Schlüter, A., Lortz, D. & Busse, F. H. 1965 On the stability of finite amplitude convection. *J. Fluid Mech.* **23**, 129–144.

Schmidt, R. J. & Saunders, O. A. 1938 On the motion of a fluid heated from below. *Proc. Roy. Soc.* A **165**, 216–228.

SOMERSCALES, E. F. C. & DOUGHERTY, T. S. 1970 Observed flow patterns at the initiation of convection in a horizontal liquid layer heated from below. *J. Fluid Mech.* **42**, 755–768.

SOMERSCALES, E. F. C. & DROPKIN, D. 1966 Experimental investigation of the temperature distribution in a horizontal layer of fluid heated from below. *Int. J. Heat Mass Transfer*, **9**, 1189–1204.

SOMERVILLE, R. C. J. 1970 Heat transfer in steady two-dimensional Bénard convection. *Notes on the* 1970 *Summer Study Program in Geophysical Fluid Dynamics, Woods Hole Oceanographic Institution Rep.* no. 70–50, I, 87–89.

WILLIS, G. E. & DEARDORFF, J. W. 1965 Measurements on the development of thermal turbulence in air between horizontal plates. *Phys. Fluids*, **8**, 2225–2229.

WILLIS, G. E. & DEARDORFF, J. W. 1967 Confirmation and renumbering of the discrete heat flux transitions of Malkus. *Phys. Fluids*, **10**, 1861–1866.

WILLIS, G. E. & DEARDORFF, J. W. 1970 The oscillatory motions of Rayleigh convection. *J. Fluid Mech.* **44**, 661–672.

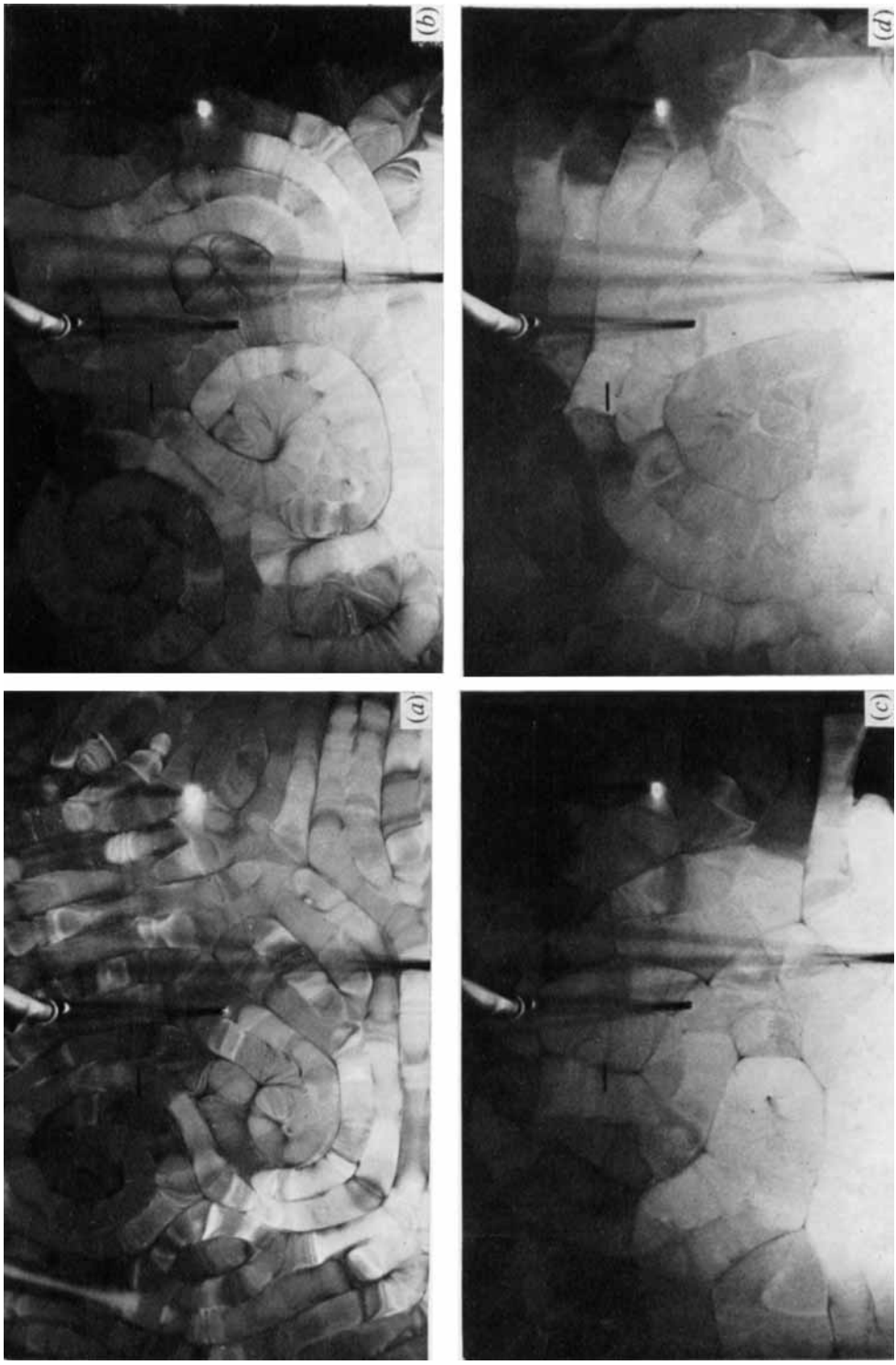

FIGURE 3. Convection patterns in air for various Rayleigh numbers. (*a*) $R = 2500$, (*b*) $R = 4000$, (*c*) $R = 6200$, (*d*) $R = 8750$. The black scale length is equal to the chamber depth h. The closest two side walls lie within $3h$ from the bottom and left-hand side of each photograph.

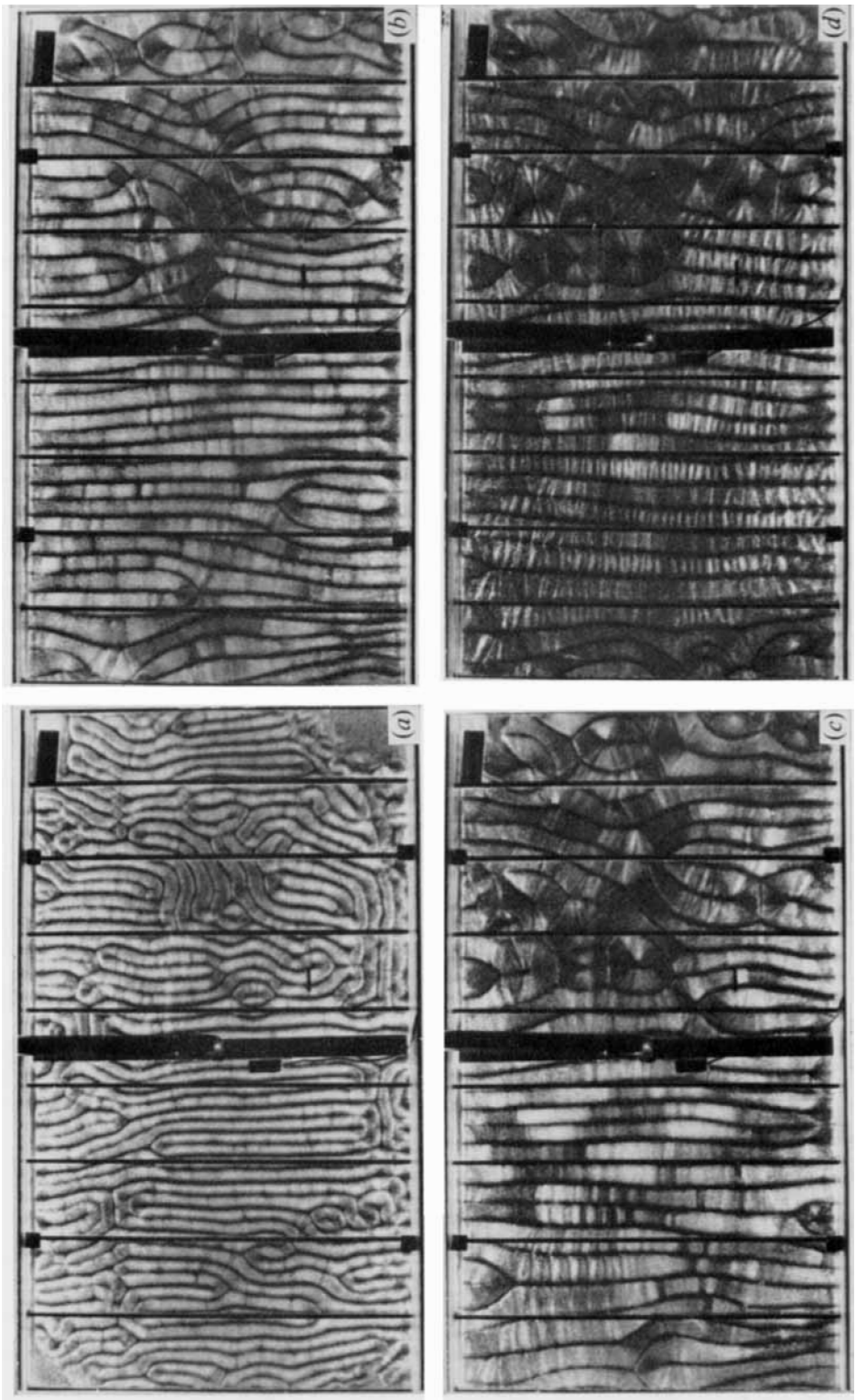

FIGURE 5. Convection patterns in water for various Rayleigh numbers. (*a*) $R = 2100$, (*b*) $R = 11000$, (*c*) $R = 17500$, (*d*) $R = 29000$. The black scale length is equal to the chamber depth. The entire chamber is viewed except for a width of $6h$ on the left- and right-hand sides.

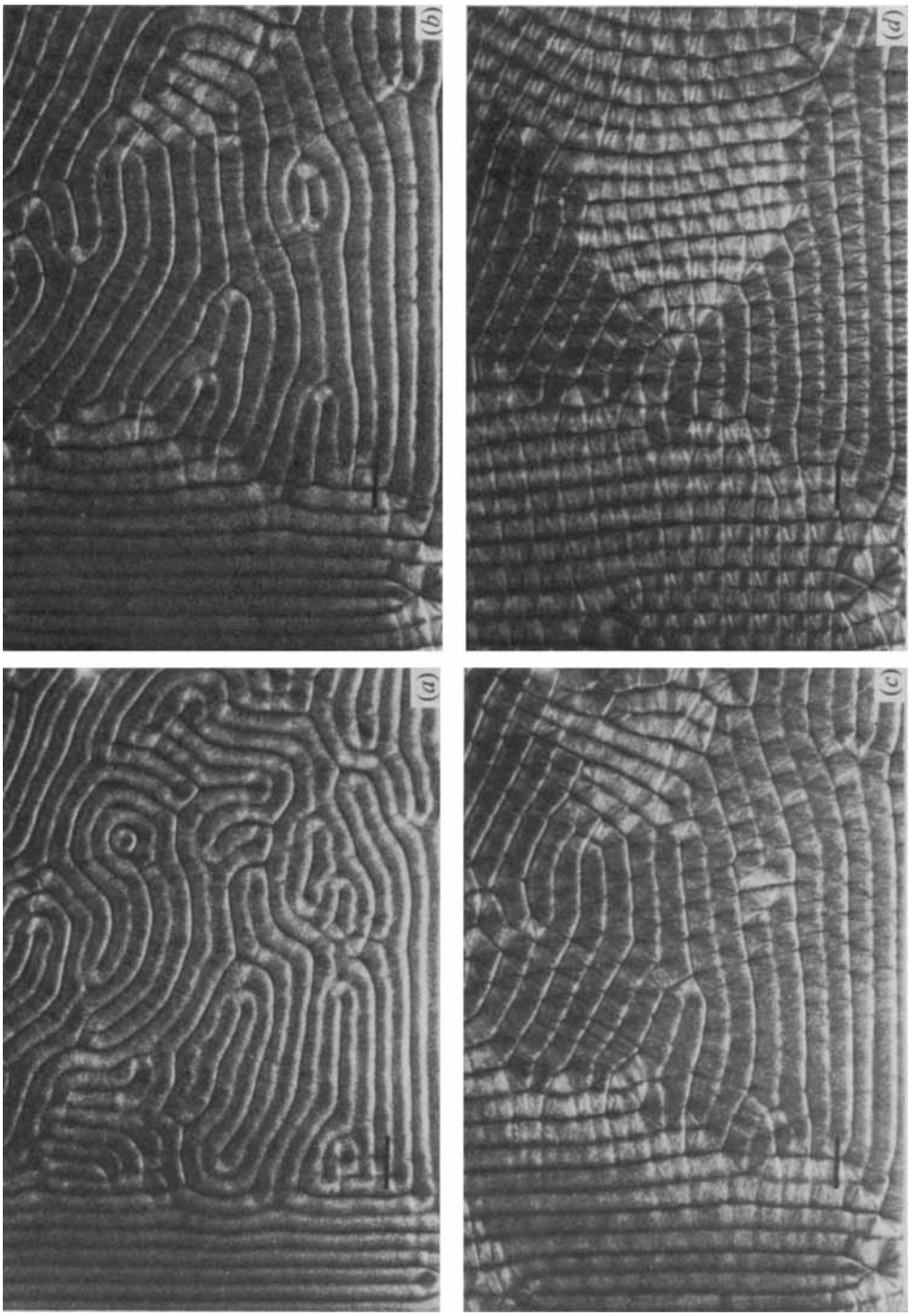

FIGURE 8. Convection patterns in silicone oil for various Rayleigh numbers. (*a*) $R = 5800$, (*b*) $R = 14000$, (*c*) $R = 19000$, (*d*) $R = 28000$. The black scale length is $2{\cdot}85h$. The closest two side walls lie within $4h$ from the bottom and $2h$ from the left-hand side of each photograph.